A self-powered vibration sensor based on electrospun poly(vinylidene fluoride) nanofibres with enhanced piezoelectric response

2016 Smart Mater. Struct. 25 105010

(http://iopscience.iop.org/0964-1726/25/10/105010)

IOP Publishing Smart Materials and Structures
Smart Mater. Struct. **25** (2016) 105010 (8pp) doi:10.1088/0964-1726/25/10/105010

A self-powered vibration sensor based on electrospun poly(vinylidene fluoride) nanofibres with enhanced piezoelectric response

Xumin Pan, Zhao Wang, Zilan Cao, Shenqiu Zhang, Yahua He, Youdong Zhang, Kansong Chen, Yongming Hu and Haoshuang Gu

Hubei Collaborative Innovation Center for Advanced Organic Chemical Materials—Hubei Key Laboratory of Ferro & Piezoelectric Materials and Devices, Faculty of Physics & Electronic Sciences, Hubei University, Wuhan, 430062, People's Republic of China

E-mail: wangzhao33@hotmail.com

Received 12 April 2016, revised 20 July 2016
Accepted for publication 14 August 2016
Published 16 September 2016

Abstract

The development of self-powered vibration sensors using polymeric piezoelectric nanomaterials has attracted great attention owing to their outstanding flexibility and energy harvesting behaviours. In this study, ultra-long poly (vinylidene fluoride) (PVDF) nanofibres with optimised β-phase content were synthesised through electrospinning method with different DC voltages. The increase in the β-phase content of the PVDF nanofibres greatly enhanced their piezoelectric response with nearly tripled output voltage and current under the same strain condition. Moreover, the output voltage exhibited linear correlations with both the amplitude and frequency of the strain. Under a fixed frequency of 1.54 Hz, the output voltage exhibited a linear correlation to the strain amplitude with strain sensitivity up to 0.92 V rad^{-1} and 0.61 V mm^{-1}. The frequency-dependent strain sensing behaviour also confirmed the necessity for frequency calibration to the measured results of vibration. Accordingly, the sensor can be used for self-powered monitoring of the vibration state of a metal foil and measuring the intrinsic resonance frequency of the objects without any powering source.

S Online supplementary data available from stacks.iop.org/SMS/25/105010/mmedia

Keywords: piezoelectric, vibration sensor, self-powered, nanofibres, PVDF

(Some figures may appear in colour only in the online journal)

1. Introduction

The detection of vibration is an important issue for monitoring the structural deformation of high-rise buildings and the working state of mechanical equipment [1]. However, traditional vibration sensors, such as piezoresistive film and optical devices, still need to be powered by an external power unit such as lion-batteries or power supply lines [2, 3]. These complex and large power supply units seriously limit the miniaturisation of sensor systems and the development of wireless sensor networks [4, 5].

Currently, self-powered vibration sensors based on piezoelectric nanowires have attracted great attention owing to their electromechanical energy harvesting behaviour to multiple kinds of mechanical energies, such as sound waves, water/air flow and movement of human bodies [6–14]. For instance, inorganic semiconductive (e.g. ZnO, InN and ZnS) nanowires have been extensively investigated as energy harvesting materials, due to their simple fabrication and large-scale integration technique [15]. Moreover, perovskite piezoelectric materials such as $Pb(Zr,Ti)O_3$, $Pb(Mg,Nb)O_3$-$PbTiO_3$ and $(K,Na)NbO_3$ that have outstanding piezoelectric

properties, have also exhibited great potential for building high-performance energy harvesters and self-powered vibration sensors [16–18]. However, these inorganic nanowires have poor flexibility, which makes them too brittle to withstand high strain and decreases the durability of the devices.

In comparison to inorganic piezoelectric materials, piezoelectric polymers such as poly(vinylidene fluoride) (PVDF), poly(vinyl chloride), poly(vinyl fluoride) and odd nylons possess higher flexibility, and thus, can tolerate larger mechanical deformation [19–21]. Among these, PVDF has exhibited relatively higher piezoelectric coefficients, as well as better mechanical flexibility, chemical stability and biocompatibility [8, 22, 23]. Film-based PVDF transducers have already been used for the self-powered monitoring of composite structures [24, 25]. Compared with films, the electrospun nanofibres (NFs) were reported to have higher energy conversion efficiency in power generation devices owing to their better flexibility [19, 26]. The electrospinning process also provides a one-step method to obtain piezoelectric PVDF NFs because the phase transition from the non-polarised α-phase to the polarised β-phase can be synchronously realised under the applied high direct-current (DC) electrical field [22, 27, 28]. For instance, both near-field and far-field electrospinning method (FFES) have been used for fabricating the PVDF NFs and the piezoelectric energy harvesters [21, 23, 29]. The devices exhibited repeatable and consistent piezoelectric voltage output, which is higher than that of the PVDF thin films. However, the commonly used electrospinning method could only result in the partially phase transition to the polarised β-phase, which limited the piezoelectric performance of the PVDF NFs as well as the energy conversion efficiency of the energy harvesters. In addition, the self-powered strain sensing performance of the PVDF NFs under different vibration states still needs to be studied in detail, although their performance as a piezoelectric nanogenerator have already been demonstrated.

As reported, the content of β-phase in PVDF NFs can be slightly modified by adjusting the content of additives in the electrospinning precursor solutions [30, 31]. In this study, an obvious increase of the β-phase content in the well-aligned PVDF NFs prepared by FFES method was realised by modifying the electrospinning voltage during the fabrication process, which greatly enhanced the piezoelectric response of the NFs with nearly tripled output voltage and current value. Subsequently, a flexible vibration sensor was fabricated, of which the detailed strain sensing performance was investigated. The devices could be utilised to monitor the amplitude and frequency of the vibration synchronously through the spontaneous output voltage up to 1.5 V. Moreover, the frequency response characteristics of the sensor were also investigated.

2. Materials and methods

2.1. Electrospinning of the PVDF NFs

The PVDF powder (MW 534000) as raw material was purchased from Sigma-Aldrich. Absolute acetone and N,N-dimethylformamide (DMF) were purchased from Sinopharm Chemical Reagent Co., Ltd (Shanghai, China). Reagents were analytical grade and used as received without further purification. PVDF solutions (12%wt) were prepared by adding 1.2 g PVDF powder to the DMF-acetone solvent mixture of 10 ml (3/7 v/v). The mixture was then stirred magnetically at 80 °C for 3 h to obtain the homogeneous PVDF precursor solution. After that, the transparent PVDF precursor solution was transferred into a Hamilton 5 ml syringe fixed onto a syringe pump (LongerPump TJP-3A/W0109-1B). The inner diameter of the needle was 0.41 mm. A DC voltage varying from 11 to 17 kV (Betran DC high voltage power supply system) was then applied between the syringe needle on the sample collector to eject the precursors from the needle with the injection speed of 50 μl min^{-1}. The sample collector consisted of two pieces of ground aluminium foil (with a gap of 2.5 mm) on a flat Teflon board that was placed 15 cm away from the needle. Finally, the collected NFs were placed in front of a bath heater for 1 h to remove excess solvent.

2.2. Fabrication of the flexible vibration sensor

The PVDF NFs were collected by a silicon wafer and then transferred to a flexible polydimethylsiloxane (PDMS) substrate. After that, a layer of platinum interdigital electrodes (IDEs) was deposited onto the NFs through magnetron sputtering method by using a pre-patterned shadow mask. The distance between the electrode stripes was 0.5 mm. After wire leading with a pair of pins, the device was further packaged using the PDMS. Finally, the completed device was immersed in methyl silicone oil and electrically poled by applying a DC voltage of 10 kV between the two electrodes for 30 min After poling, the electrodes were shorted for over 12 h to eliminate the stored charges.

2.3. Measurement and characterisation

The structure of the product was characterised by x-ray diffraction (XRD, Bruker D8 Advance, CuKα, $\lambda = 0.154\,06$ nm) and Fourier transform infra-red spectroscopy (FTIR, Thermo Fisher Scientific, Nicolet iS10). The surface morphology was characterised by field emission scanning electron microscopy (FE-SEM, JEOL JSM7100F). The vibration sensing test was performed using a vibration generator (Shanghai Zhu Rui ATLC, JZ-1) with the signal generated by a function arbitrary waveform generator (UNI-T, UTG2000A) and a power amplifier (Shanghai Zhu Rui ATLC, GF-10W). The device's piezoelectric data was measured using a data acquisition card (National Instruments, NI USB-6210).

3. Results and discussion

3.1. Preparation and characterisation of PVDF NFs

The PVDF NFs were synthesised using the FFES method with a pair of parallel aluminium foils as the collector. As shown in figures 1(a) and S1, the electrical field distribution

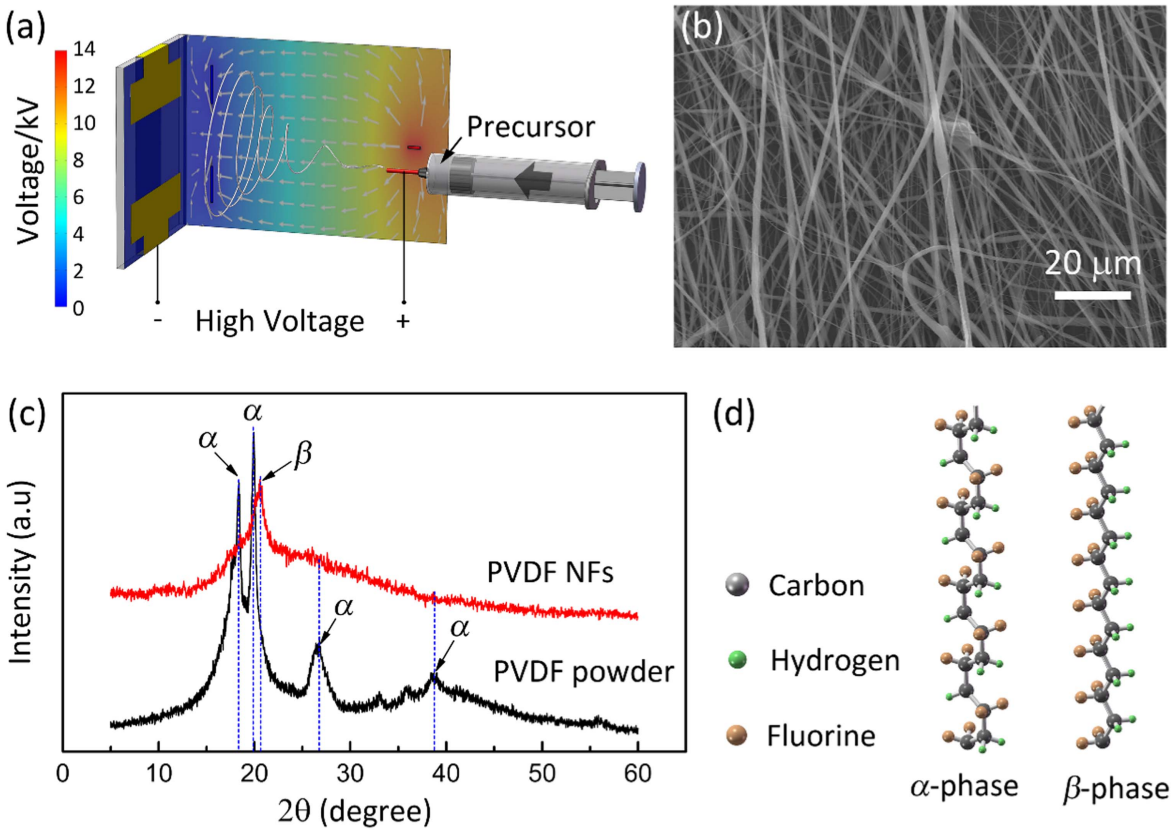

Figure 1. (a) Schematic diagram of the electrospinning process of PVDF NFs showing the finite element analysis results of the electrical field distribution between the needle and the sample collector. The detailed simulation parameters were described in the supplementary information. (b) FE-SEM image of the as-synthesised PVDF NFs. (c) XRD patterns of the as-synthesised PVDF NFs and the precursor PVDF powder. (d) The molecule chain structure of α-phase and β-phase PVDFs.

between the positive needle and the negative Al collectors make the ejected NFs swing between the parallel Al foils, which could lead to the improvement of alignment of the NFs [32]. Figure 1(b) shows the FE-SEM image of the as-synthesised NFs with electrospinning voltage of 14 kV. Most of the PVDF NFs are well aligned towards the vertical direction and exhibited much better alignment than the NFs synthesised by using a flat Al collector (shown in figure S2). Moreover, the XRD results confirmed that the molecular structure of the PVDF NFs was transformed from pure α-PVDF to a mixed phase of both α- and β-PVDF with β-PVDF as the major phase. As shown in figure 1(c), the XRD patterns of PVDF NFs have a distinct peak located at $2\theta = 20.7°$, which is the characteristic peak of the (110) face of β-PVDF [33]. Meanwhile, the broad peak shoulder also suggests the existence of α-PVDF in the NFs with diffraction peaks at $2\theta = 18.4°$ (020), 19.9° (021), 27.8° (021) and 38.4° (002). The phase transition of the NFs after the electrospinning treatment is attributed to the stretching behaviour of the NFs and the stimulation of the applied high electrical field. Figure 1(d) shows a schematic diagram of the molecular chain structure of both phase PVDFs. The β-PVDF exhibits obvious molecular polarisation due to the ordered arrangement of C–H and C–F bonds, which makes them suitable to be applied as piezoelectric materials without further poling treatment.

In order to study the impact of electrospinning voltage on the piezoelectric performance of the PVDF NFs, various samples were prepared with different DC voltages applied between the needle and sample collector. Firstly, the FE-SEM images shown in figure S3 confirm that the NFs can only be obtained when the DC voltage is set in the range of $9 \sim 17$ kV. Changes in the DC voltage have a great impact on the diameter of the NFs due to the changed driving force that stretches the precursor to NFs. Moreover, the XRD and FTIR results shown in figure 2 suggest that the content of β-PVDF were changed when the DC voltage was increased. As shown in figure 2(a), the intensity of the diffraction peaks at $2\theta = 20.7°$ first increased when the DC voltage was increased from 11 to 15 kV, which could be attributed to the increased stretching force and electrical field at this higher voltage condition. However, the peak intensity decreased when the voltage was increased further. The same conclusion was obtained from the FTIR results. As shown in figure 2(b), the FTIR bands at 613, 764 and 976 cm^{-1} are characteristic bands of α-PVDF, while bands at 840 and 1284 cm^{-1} are ascribed to β-PVDF [34]. Based on the FTIR results, the content of β-PVDF in the NFs can be calculated as

$$F(\beta) = \frac{X_\beta}{X_\alpha + X_\beta} = \frac{A_\beta}{(K_\beta/K_\alpha)A_\alpha + A_\beta}, \quad (1)$$

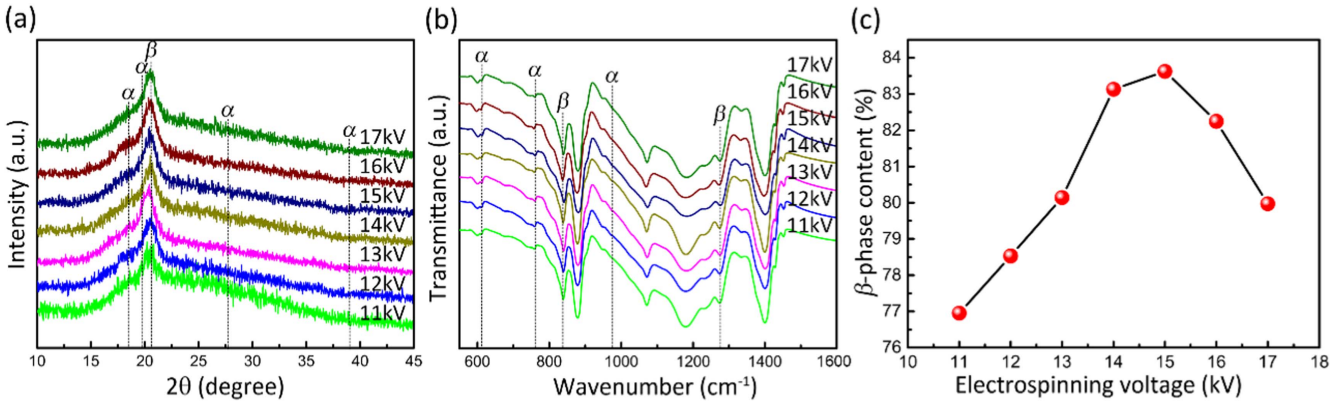

Figure 2. The XRD patterns (a) and FTIR spectrums (b) of the PVDF NFs synthesised with different electrospinning voltages. (c) The β-phase content as a function of the electrospinning voltage according to the FTIR results.

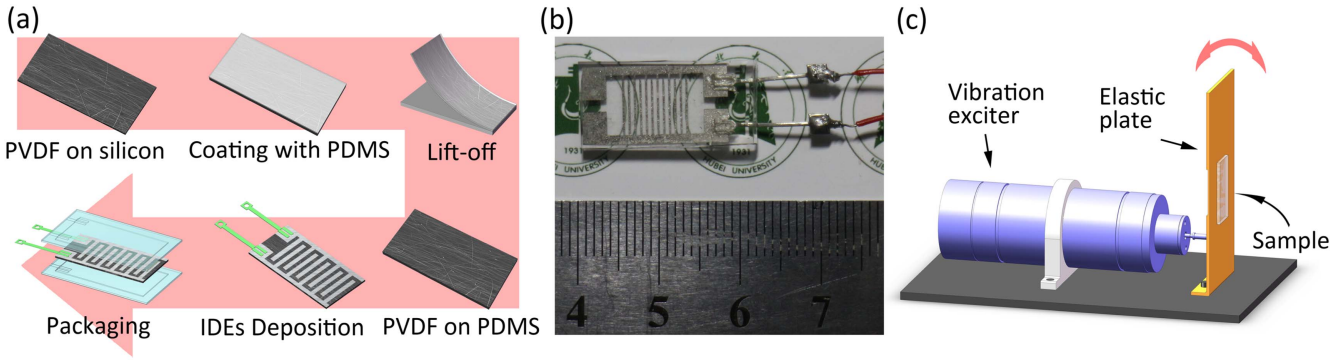

Figure 3. A schematic diagram of the fabrication process (a), the photo image (b) and a schematic diagram of the vibration generation method (c) of the flexible vibration sensor based on PVDF NFs.

where A_α and A_β are the absorbance at 764 and 840 cm^{-1}, respectively, and K_α and K_β are the absorption coefficients, which are 6.1×10^4 and 7.7×10^4 $cm^2\,mol^{-1}$, respectively. According to the calculation result shown in figure 2(c), the NFs obtained at 15 kV contain the highest content (83.6%) of β-PVDF. Increasing the DC voltage further leads to a decrease in the content of β-PVDF, due to the corona discharge and instability of the electric field force at ultra-high voltage conditions during the electrospinning process [35].

3.2. Vibration sensing performance

Figures 3(a) and (b) show the fabrication process and a photo image, respectively, of the flexible vibration sensor based on the PVDF NFs. The PVDF NFs were transferred from the Si substrate onto the flexible PDMS film though a simple lift-off process. After the deposition of IDEs and wire leading by conducting pins, the whole device was packaged by PDMS to protect the NFs from physical damage and chemical contamination. As shown in figure 3(b), the as-fabricated device was approximately $2.0 \times 1.0 \times 0.3$ cm^3 in dimension and exhibited high transparency to visible light. After poling treatment, the flexible sensor was pasted on the root section of a bronze foil with 0.2 mm thickness. As shown in figure 3(c), the bronze foil was fixed at the root and stimulated to vibrate by a vibration exciter to induce the bending motion of the flexible sensor. Figures 4(a) and (b) show the open-circuit voltage and short-circuit current generated by the sensor with different β-PVDF content when the bronze foils were vibrating with the same frequency and amplitude. All sensors exhibited obvious piezoelectric energy harvesting behaviour. The impulsive and alternative voltage signal generated by the sensors are attributed to the continuous switching behaviour of the PVDF NFs between the stretching and compressing states during the vibration process. This then generates reverse piezoelectric potential along the axial direction of the NFs and forces the electrons in the external circuit to move forwards and backwards between the electrodes [18]. The results also confirm that the piezoelectric response of the sensor can be greatly improved when the β-phase content is increased. As shown in figure 4(c), the peak-to-peak voltage (V_{pp}) of the sensor with the highest β-phase content (83.6%) is ~2.3 V, which is nearly three times higher than the V_{pp} value of the sensor with β-phase content of 76.9% (~0.8 V). The same tendency could also be found for the peak-to-peak value of current with the changing of β-phase content. These performance enhancements are mainly attributed to the increased piezoelectric constant of the PVDF NFs with higher content of polarised β-phase. It is worth noting that the piezoelectric response of PVDF NFs with optimised β-phase content are comparable to reported values in the literature of traditional perovskite oxide-based NFs such as $Pb(Zr,Ti)O_3$ and $(K,Na)NbO_3$ [18, 36].

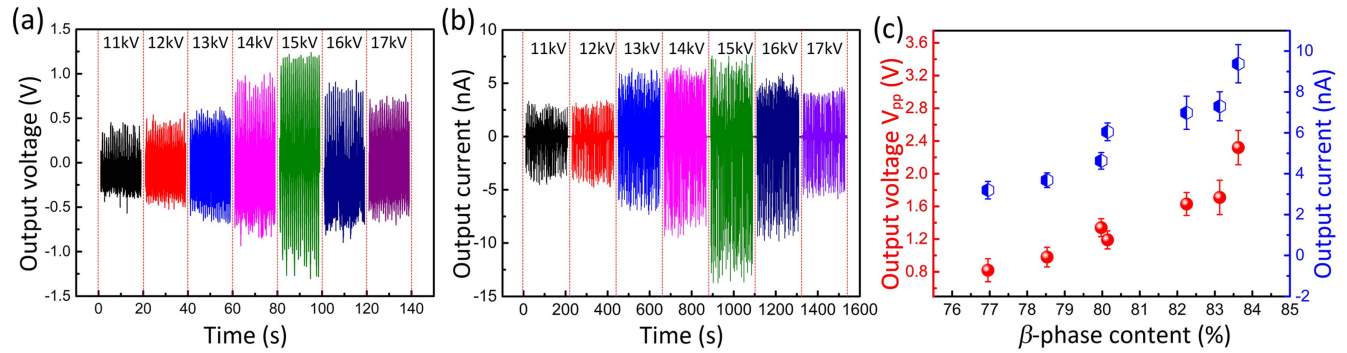

Figure 4. The energy harvesting performance of the flexible vibration sensor based on PVDF NFs with different β-phase content. (a) The open-circuit voltage. (b) The short-circuit current. (c) The peak-to-peak voltage and current as a function of β-phase content.

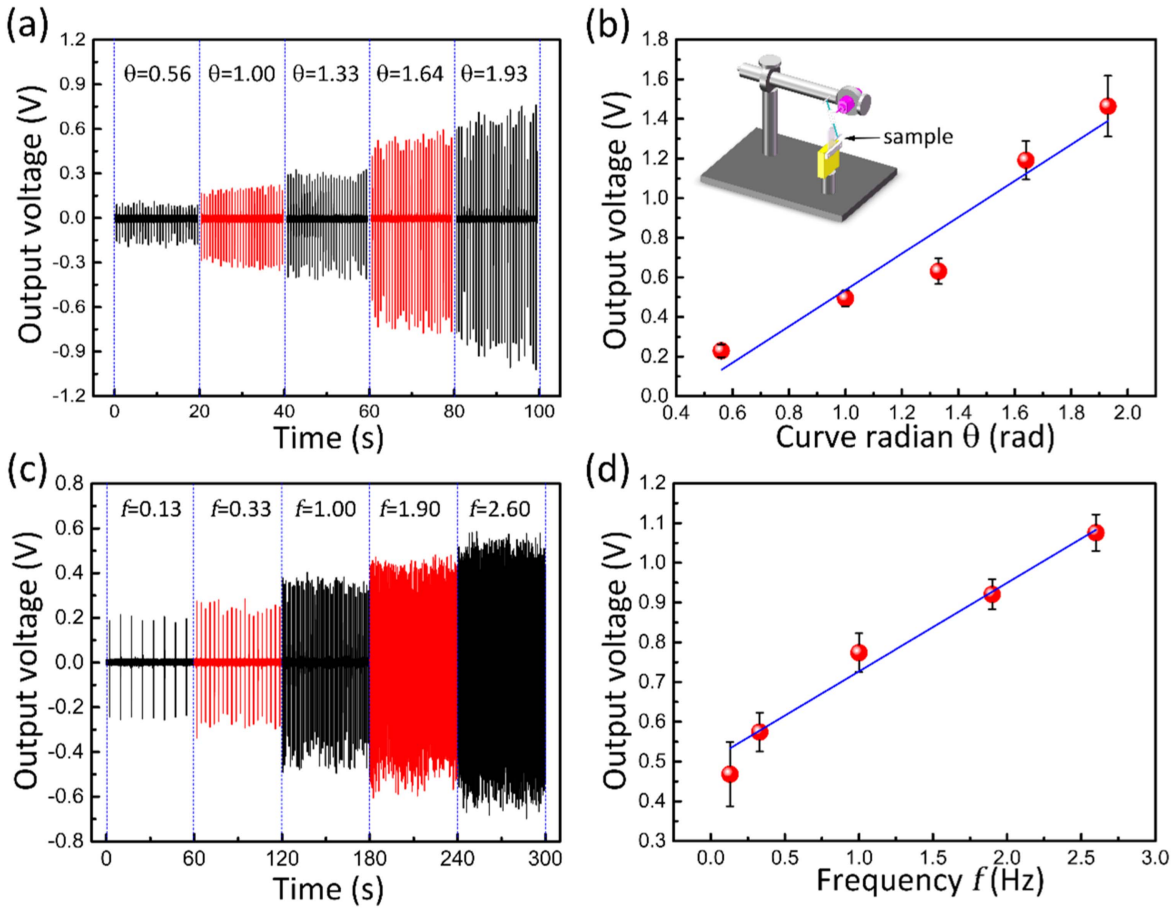

Figure 5. The output voltage generated by the flexible PVDF vibration sensor under different conditions when the sensor was bent by a rotating stiff stick. (a) The output voltage of the sensor with the curve radian (θ) varying from 0.56 to 1.93 rad, which represents the axial strain of the nanofibres. (b) The peak value of output voltage as a function of curve radian. (c) The output voltage of the sensor with the strain frequency varying from 0.13 to 2.60 Hz. (d) The peak value of output voltage as a function of strain frequency.

Figure 5 shows the characterisation results of the vibration sensing performance for the flexible sensor with the highest β-phase content. As shown by the inset picture in figure 5(b), a rotating stiff stick was used to induce the bending deformation on the sensor. The strain amplitude and frequency of the sensor was controlled by adjusting the length and rotating speed of the stick, respectively. The curve radian and axial deformation of the sensor was calculated by assuming that the sensor was uniformly bent during the testing process. As shown in figures 5(a) and (b) and S4, the average value of V_{pp} linearly increased from ~0.23 to 1.46 V under a frequency of ~1.54 Hz when the curve radian and axial deformation of the sensor were increased from 0.56 to 1.93 rad and 0.84 to 2.90 mm, respectively. Accordingly, the sensitivity of the flexible vibration sensor was approximately 0.92 V rad^{-1} and 0.61 V mm^{-1} according to the linear fitting result. Moreover, the frequency-dependent output voltage was also measured with the fixed curve radian. Owing to the

switching behaviour of the output voltage shown in figure 5(c), the frequency of strain can be directly calculated as being between 0.13 and 2.60 Hz by counting the time-interval between the adjacent voltage peaks. As shown in figure 5(d), the average value of V_{pp} also linearly increased with the strain frequency when the curve radian was fixed at ~1.5 rad. Both the linearly increased output voltage with the strain amplitude and frequency agreed with fundamental piezoelectric theory, where the piezoelectric potential generated by the strain piezoelectric materials is linearly correlated with the strain and strain rate [18]. Meanwhile, these results also suggest that the self-powered vibration sensing result obtained from the sensor should be calibrated according to the calculated strain frequency to guarantee the accuracy of the measurement results.

Based on the characterisation of the vibration sensing performance, two typical applications of the self-powered flexible sensor were carried out. Figure 6(a) shows the output voltage generated by the flexible sensor pasted onto a vibrating bronze foil, which was initially triggered at a certain degree and then released to move under elastic restoring and damping force. Firstly, the decrease of voltage amplitude clearly demonstrates the dynamic damping motion of the bronze foil. According to piezoelectric and vibration theory, the output voltage can be attributed to a function as

$$V = C_0 A_0 e^{-\beta t} \cos(\omega t + \varphi), \quad (2)$$

where C_0 is the piezoelectric parameters of the PVDF NFs, A_0 and φ are the initial amplitude and phase angle determined by the initial triggering condition, respectively, ω is the vibration angular frequency of the bronze foil and β is the damping factor [37]. By fitting the peak value of output voltage with the exponential function of $A_0 e^{-\beta t}$, the damping factor was calculated as 0.16. Figure 6(b) shows that the vibration frequency of the bronze foil which was calculated by taking the reciprocal of the adjacent peak time difference was gradually decreased from 1.79 to 1.06 Hz from 86 to 96 s. Furthermore, the Fourier transformation result of the voltage signals shown in figure 6(c) confirmed the primary vibration frequency and angular frequency of the bronze foil were ~1.47 Hz and ~9.24 rad s^{-1}, which is agree with the calculated result from figure 6(b). Therefore, the vibration sensor can be used for monitoring both the amplitude and the frequency of the vibrating object without any powering sources.

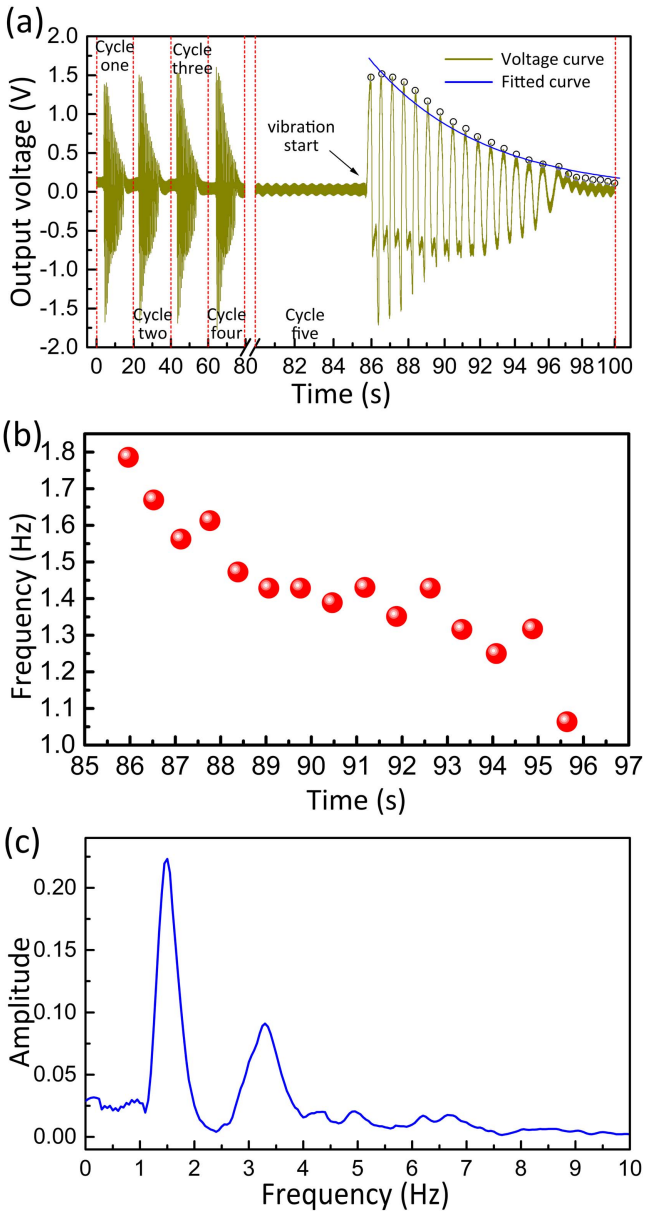

Figure 6. The vibration sensing performance of the flexible sensor pasted onto a bronze foil 0.2 mm in thickness, which was fixed at one end. (a) The output voltage of the sensor when the bronze foil was bent to a certain degree and released for free vibrating. (b) The vibration frequency calculated from the voltage curve. (c) Frequency spectrogram calculated by Fourier transform.

Figure 7(a) shows the output voltage of the flexible sensor when the bronze foil was stimulated by a vibration exciter with frequencies sweeping from 5 to 30 Hz. As shown, there is no obvious voltage output was found as the frequency was increased from 5 to 15 Hz. After that, the output voltage was increased to the maximum value and then decreased with further increased frequency, which clear demonstrated the resonance behaviour of the bronze foil. Figure 7(b) shows the enlarged view of the figure 7(a) from 17.5 to 18.5 s. The highest output voltage could be found at ~17.88 s. By counting the time interval between the adjacent voltage peak (~0.052 s), the vibration frequency of the bronze foil could be calculated as ~19.23 Hz. This value agrees with the frequency of the vibration exciter (~19.88 s) with a small deviation of ~3%, which suggested that the sensor could be used for the measuring of resonance behaviour of the objects. Furthermore, the variation of output voltage during the frequency sweeping process could also be used for measuring the vibration amplitude after further frequency-calibrations. The highly flexible device with both flexible substrate and piezoelectric NFs provides great potential in long-term application as the strain sensors rather than the traditional ZnO and perovskite oxide materials.

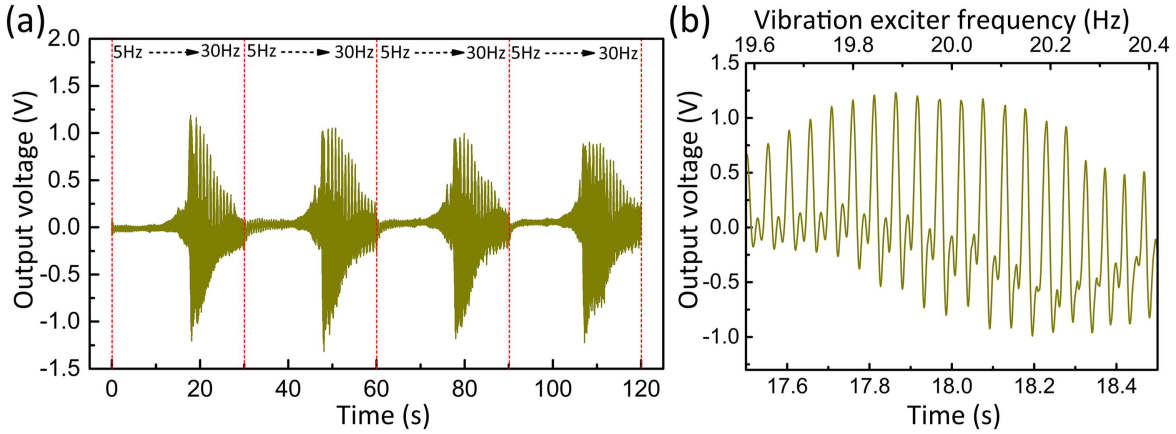

Figure 7. (a) The vibration sensing performance of the flexible sensor pasted onto a bronze foil when the foil was vibrating under the stimulation of different frequencies. (b) The enlarged view of voltage curve from 17.5 to 18.5 s.

4. Conclusion

Well-aligned PVDF NFs with various β-phase content were synthesised using the FFES method with different electrospinning voltages. A flexible piezoelectric self-powered vibration sensor was fabricated by transferring the PVDF NFs from silicon to PDMS substrate. The piezoelectric output voltage generated by the sensor was increased by nearly two times when the β-phase content of the PVDF NFs was increased from 76.9% to 83.6%. The enhancement of the piezoelectric response of PVDF NFs could greatly increase the sensitivity of self-powered sensors. Moreover, output voltage generated by the sensor with a β-phase content of 83.6% exhibited linear correlations with both the strain amplitude and frequency. Its sensitivity to the bending strain with frequency of ~1.54 Hz was approximately 0.92 V rad^{-1} and 0.61 V mm^{-1}. This result confirmed the necessity for frequency calibration of the sensing results. Based on the self-powered vibration sensing behaviour, the flexible sensor could be used for self-powered monitoring of the vibration state of a metal foil and measuring the intrinsic resonance frequency of objects without any powering source.

Acknowledgments

This work was financially supported by the National Science Foundation of China (Grant Nos. 11504099, 11474088, 11274103) and the Applied Basic Research Project of Wuhan (Grant No. 2014010101010006).

References

[1] Chen J, Zhu G, Yang W, Jing Q, Bai P, Yang Y, Hou T C and Wang Z L 2013 Harmonic-resonator-based triboelectric nanogenerator as a sustainable power source and a self-powered active vibration sensor *Adv. Mater.* **25** 6094–9

[2] Patil S J, Duragkar N and Rao V R 2014 An ultra-sensitive piezoresistive polymer nano-composite microcantilever sensor electronic nose platform for explosive vapor detection *Sensors Actuators* B **192** 444–51

[3] Xu B, Li Y, Sun M, Zhang Z-W, Dong X-Y, Zhang Z-X and Jin S-Z 2012 Acoustic vibration sensor based on nonadiabatic tapered fibers *Opt. Lett.* **37** 4768–70

[4] Wang S, Mu X, Yang Y, Sun C, Gu A Y and Wang Z L 2015 Flow-driven triboelectric generator for directly powering a wireless sensor node *Adv. Mater.* **27** 240–8

[5] Lee M, Bae J, Lee J, Lee C-S, Hong S and Wang Z L 2011 Self-powered environmental sensor system driven by nanogenerators *Energy Environ. Sci.* **4** 3359–63

[6] Wang Z L, Chen J and Lin L 2015 Progress in triboelectric nanogenerators as a new energy technology and self-powered sensors *Energy Environ. Sci.* **8** 2250–82

[7] Wang X, Wang S, Yang Y and Wang Z L 2015 Hybridized electromagnetic–triboelectric nanogenerator for scavenging air-flow energy to sustainably power temperature sensors *ACS Nano* **9** 4553–62

[8] Fuh Y-K, Chen P-C, Huang Z-M and Ho H-C 2015 Self-powered sensing elements based on direct-write, highly flexible piezoelectric polymeric nano/microfibers *Nano Energy* **11** 671–7

[9] Yang J, Chen J, Liu Y, Yang W, Su Y and Wang Z L 2014 Triboelectrification-based organic film nanogenerator for acoustic energy harvesting and self-powered active acoustic sensing *ACS Nano* **8** 2649–57

[10] Alluri N R, Saravanakumar B and Kim S-J 2015 Flexible, hybrid piezoelectric film (BaTi $(1-x)$ Zr_x O_3)/PVDF nanogenerator as a self-powered fluid velocity sensor *ACS Appl. Mater. Interfaces* **7** 9831–40

[11] Sun C, Shi J, Bayerl D J and Wang X 2011 PVDF microbelts for harvesting energy from respiration *Energy Environ. Sci.* **4** 4508–12

[12] Zeng W, Tao X-M, Chen S, Shang S, Chan H L W and Choy S H 2013 Highly durable all-fiber nanogenerator for mechanical energy harvesting *Energy Environ. Sci.* **6** 2631–8

[13] Delnavaz A and Voix J 2014 Flexible piezoelectric energy harvesting from jaw movements *Smart Mater. Struct.* **23** 105020

[14] Guigon R, Chaillout J-J, Jager T and Despesse G 2008 Harvesting raindrop energy: experimental study *Smart Mater. Struct.* **17** 015039

[15] Xu S, Qin Y, Xu C, Wei Y, Yang R and Wang Z L 2010 Self-powered nanowire devices *Nat. Nanotechnol.* **5** 366–73

[16] Bai S, Xu Q, Gu L, Ma F, Qin Y and Wang Z L 2012 Single crystalline lead zirconate titanate (PZT) nano/micro-wire based self-powered UV sensor *Nano Energy* **1** 789–95

[17] Xu S, Yeh Y-W, Poirier G, McAlpine M C, Register R A and Yao N 2013 Flexible piezoelectric PMN–PT nanowire-based nanocomposite and device *Nano Lett.* **13** 2393–8
[18] Wang Z, Zhang Y, Yang S, Hu Y, Wang S, Gu H, Wang Y, Chan H and Wang J 2015 (K, Na) NbO_3 nanofiber-based self-powered sensors for accurate detection of dynamic strain *ACS Appl. Mater. Interfaces* **7** 4921–7
[19] Soin N, Shah T H, Anand S C, Geng J, Pornwannachai W, Mandal P, Reid D, Sharma S, Hadimani R L and Bayramol D V 2014 Novel '3D spacer' all fibre piezoelectric textiles for energy harvesting applications *Energy Environ. Sci.* **7** 1670–9
[20] Liu Z, Xu J, Chen D and Shen G 2015 Flexible electronics based on inorganic nanowires *Chem. Soc. Rev.* **44** 161–92
[21] Lee C and Tarbutton J A 2014 Electric poling-assisted additive manufacturing process for PVDF polymer-based piezoelectric device applications *Smart Mater. Struct.* **23** 095044
[22] Soin N, Boyer D, Prashanthi K, Sharma S, Narasimulu A, Luo J, Shah T, Siores E and Thundat T 2015 Exclusive self-aligned β-phase PVDF films with abnormal piezoelectric coefficient prepared via phase inversion *Chem. Commun.* **51** 8257–60
[23] Fang J, Niu H, Wang H, Wang X and Lin T 2013 Enhanced mechanical energy harvesting using needleless electrospun poly (vinylidene fluoride) nanofibre webs *Energy Environ. Sci.* **6** 2196–202
[24] da Silva A B, Arjmand M, Sundararaj U and Bretas R E S 2014 Novel composites of copper nanowire/PVDF with superior dielectric properties *Polymer* **55** 226–34
[25] Kim Y-S, Xie Y, Wen X, Wang S, Kim S J, Song H-K and Wang Z L 2015 Highly porous piezoelectric PVDF membrane as effective lithium ion transfer channels for enhanced self-charging power cell *Nano Energy* **14** 77–86
[26] Fuh Y-K, Ye J-C, Chen P-C, Ho H-C and Huang Z-M 2015 Hybrid energy harvester consisting of piezoelectric fibers with largely enhanced 20 V for wearable and muscle-driven applications *ACS Appl. Mater. Interfaces* **7** 16923–31
[27] Baji A, Mai Y-W, Li Q and Liu Y 2011 Electrospinning induced ferroelectricity in poly (vinylidene fluoride) fibers *Nanoscale* **3** 3068–71
[28] Ahn Y, Lim J Y, Hong S M, Lee J, Ha J, Choi H J and Seo Y 2013 Enhanced piezoelectric properties of electrospun poly (vinylidene fluoride)/multiwalled carbon nanotube composites due to high β-phase formation in poly (vinylidene fluoride) *J. Phys. Chem.* C **117** 11791–9
[29] Chang C, Tran V H, Wang J, Fuh Y-K and Lin L 2010 Direct-write piezoelectric polymeric nanogenerator with high energy conversion efficiency *Nano Lett.* **10** 726–31
[30] Andrew J and Clarke D 2008 Enhanced ferroelectric phase content of polyvinylidene difluoride fibers with the addition of magnetic nanoparticles *Langmuir* **24** 8435–8
[31] Zheng J, He A, Li J and Han C C 2007 Polymorphism control of poly (vinylidene fluoride) through electrospinning *Macromol. Rapid Commun.* **28** 2159–62
[32] Li D and Xia Y 2004 Electrospinning of nanofibers: reinventing the wheel? *Adv. Mater.* **16** 1151–70
[33] Li J, Meng Q, Li W and Zhang Z 2011 Influence of crystalline properties on the dielectric and energy storage properties of poly (vinylidene fluoride) *J. Appl. Polym. Sci.* **122** 1659–68
[34] Gregorio R and Borges D S 2008 Effect of crystallization rate on the formation of the polymorphs of solution cast poly (vinylidene fluoride) *Polymer* **49** 4009–16
[35] Shao H, Fang J, Wang H and Lin T 2015 Effect of electrospinning parameters and polymer concentrations on mechanical-to-electrical energy conversion of randomly-oriented electrospun poly (vinylidene fluoride) nanofiber mats *RSC Adv.* **5** 14345–50
[36] Chen X, Xu S, Yao N and Shi Y 2010 1.6 V nanogenerator for mechanical energy harvesting using PZT nanofibers *Nano Lett.* **10** 2133–7
[37] Yu A, Jiang P and Wang Z L 2012 Nanogenerator as self-powered vibration sensor *Nano Energy* **1** 418–23